Optik - International Journal for Light and Electron Optics 206 (2020) 164232

Contents lists available at ScienceDirect

Optik

journal homepage: www.elsevier.com/locate/ijleo

Original research article

Microscope images automatic focus algorithm based on eight-neighborhood operator and least square planar fitting

Chunmei He[a,*], Xiaorui Li[a], Yanyun Hu[a], Zhengchun Ye[b], Hongyu Kang[a]

[a] College of Computer Science and College of Cyberspace Security, Xiangtan University, Xiangtan, Hunan 411105, China
[b] College of Mechanical Engineering, Xiangtan University, Xiangtan, Hunan 411105, China

ARTICLE INFO

Keywords:
Microscope autofocus
Automatic microscope image acquisition
Eight-neighborhood operator
Least square planar fitting

ABSTRACT

An automatic focus algorithm based on eight-neighborhood operator and least square planar fitting method is proposed to acquire the three-dimensional microscope focusing images in this paper. Firstly, eight-neighborhood operator and evaluation function are presented to locate the cells in the low-power microscope images in this paper. Then the automatic focus algorithm based on eight-neighborhood operator and least square planar fitting method is given to acquire the three-dimensional microscope cell images. After that, some experiments are given in the paper. The eight-neighborhood operator is compared with the traditional evaluation function in terms of the complexity of the operation and the effect of the evaluation function. Also, comparative experiments are conducted to verify the feasibility of the automatic focus algorithm in this paper. The experimental results showed that the proposed microscope automatic focus algorithm is effective and has a good fitting degree.

1. Introduction

A computer-aided medical diagnosis can not only guarantee the objectivity and accuracy of medical diagnosis but also save the time and energy of medical experts, so the study of computer-aided medical diagnosis has very important theoretical and practical significance [1]. The automatic acquisition and recognition of microscopic cell images is an important field of computer-aided diagnosis. And the improvement of the efficiency of the automatic acquisition of microscopic cell images cannot be achieved without the rapid focus of microscopic cell images. With the development of science and technology, automatic microscope image acquisition and computer-aided image processing becomes a trend. Many researchers make progress in automatically focusing and acquiring microscope images. It's illustrated a novel approach for rapid acquisition of high-volume microscopic images used to count blood cells automatically [2]. In [3], it is proposed a method to automatically or semi-automatically perform the image selection task. The approach is based on some simple, fast and effective image quality descriptors, which can be computed during acquisition, to characterize foil-hole and data images. It is described an algorithm that can identify the centroid of single nuclear pore complexes and determine their localization relative to the distribution of lamin protein filaments in [4]. Using this algorithm, a percentage of nuclear pore complexes localized within the nuclear lamin network was accurately calculated, that could be compared between cells expressing different lamin complements. It develops an automatic measurement technique that combines a fully automated con-focal microscope with novel automatic image analysis software that was written with image processing techniques derived from the computer science field in [5]. In [6], an automated microscope was developed that mechanically focuses and captures images of the urine sediment for image recognition of four urine constituents in the urinalysis examination. In [7], a high-magnification and high-

* Corresponding author.
E-mail address: xiaoxiao_he8@163.com (C. He).

https://doi.org/10.1016/j.ijleo.2020.164232
Received 9 November 2019; Received in revised form 12 January 2020; Accepted 14 January 2020

resolution micro-image remote acquisition system of uredinispores of Puccinia striiformis f. sp. tritici is designed and manufactured. The hardware and software architectures of the micro-image remote acquisition system are designed, which realized a series of functions, including automatic supply of slide, coating a thin film of petroleum jelly, aerial urediniospore capture, urediniospore micro-image acquisition, and slide recycling. The automatic focusing and acquiring the microscope images are further researched. In this paper, an automatic focus algorithm based on the eight-neighborhood operator and the least square planar fitting method is presented. The proposed automatic focus algorithm is tested by different evaluation functions, and the experiments show the good performance of the proposed automatic focus algorithm.

The following structure of this paper is as below. In section 2, the related works of automatic microscope image acquisition and recognition are introduced. In section 3, some typical focusing evaluation functions are introduced. Section 4 presents the proposed automatic focus algorithm based on eight-neighborhood operator and the planar fitting automatic focus strategy. Section 5 gives some experiments to show the good performance of the proposed automatic focus algorithm and strategy. Section 6 gives the conclusions.

2. Related works

Optical microscope and traditional micro-cell recognition technology are still used in the acquisition and recognition of micro-cell images in many small and medium-sized hospitals. Traditional cell recognition is recognized by manual operation mainly by professionals of the hospital. According to incomplete hospital statistics, about 20 % of routine blood samples need to be reexamined. The manual operation method requires a long time to focus each time, and the medical staff is responsible for the acquisition and recognition of microscopic cell images take a lot of time, which largely wastes medical resources. According to the investigation at present in the clinical examination, the use of the ordinary optical microscope and artificial microscope in cell recognition technology is the highest.

Recently many scholars carry out lots of research on the automatic microscope and made great signs of progress. A compound automatic judgment method combining image sharpness evaluation function, modulation transfer function (MTF) and auxiliary function are proposed to improve mountaineering method [8]; the image definition evaluation function and the value of MTF are used to jointly determine the search direction jointly. A new flexural positioning machine based on multistage spring is designed in order to obtain a long focal length range [9]. An automatic focus algorithm for industrial image measurement is developed in [10]; an image sharpness evaluation based on fuzzy entropy method is proposed; also, a searching method is proposed combined with multi-scale global search and fine curve fitting to get the best-focused image. An improved automatic focus window algorithm based on the improved fish swarm selection algorithm is proposed [11]. The out-of-focus position with the sensor is detected, and the online data processing is conducted to provide feedback information for the real-time focus plane locking of the sample surface [12]. A clustering is proposed based circle fitting algorithm to calculate the radius from the reflected laser beam to the detection point as the key factor to obtain the defocus value [13]. A new radar image automatic focus algorithm for sparse driving rotating targets is proposed in [14]. A new automatic focus method is proposed based on image fusion and automatic panoramic constraint around the specimen to minimize the automatic scanning time of the microscope imaging system in [15]. Multi-focus color image fusion is proposed for the automatic focus of micro imaging. Image sequence-axis are captured by using the microscope eyepiece camera to move the microscope table along Z. A system for the identification of pollen grains in bright-field microscopic images is presented in [16]. A multi-focus image fusion method with alternating guided filtering (AGF) is proposed in [17]. Twenty-four different focus measure functions (FMFs) on the stack of thirty-one conventional microscopes field of view images obtain from three different microscopes is applied to determine the optimal focus of one of the seven FMFs with more than 90 % accuracy in [18].

In one word, research on microscope autofocus algorithm make lots of progress. However, microscopic blood cells are a specific research field, and there is no specific algorithm for focusing on microscopic blood cell images. Therefore this paper proposes a fully automatic focusing microscopy method based on the eight-neighborhood operator and least square planar fitting method. The proposed method leaves out the manual focus for cell recognition process and improves the efficiency of the cell recognition.

3. Automatic focus evaluation functions

In this section, some focusing evaluation functions are introduced. Automatic focus is the core technology of automatic microscope, which includes automatic focus evaluation function and automatic focus strategy. The function to evaluate whether an image is clear is called focusing evaluation function. When the evaluation function achieves the best effect, it is the focal position of the microscope [19,20]. The focusing evaluation functions have three characteristics: unbiasedness, unimodality, and sufficient signal-to-noise ratio [21,22]. They are described as follows.

(1) unbiasedness. When the sharpness function works best, it is the focus of the microscope.
(2) Unimodality. It indicates that the definition function has one and only one optimal point.
(3) Sufficient signal-to-noise ratio. It means that the definition function can ensure that the correct focus is found under certain interference or noise.

Typical focus evaluation functions include the variance function, Brenner function, Tennengard function and energy gradient function [2324]. These focusing evaluation functions are introduced as follows.

3.1. Variance function

The variance function is a popular autofocus function. The sharpness of the image is the sum of squares of the difference between the gray value of each pixel and its gray mean. The sharper the image, the higher the difference between the gray value and its gray mean value. Therefore, the variance function can be used as an evaluation standard for focusing on clarity. The Variance evaluation function is given by

$$f(I) = \sum_{x}\sum_{y} (I(x, y) - \mu)^2 \tag{1}$$

where μ is the average gray value of the whole image.

3.2. Brenner evaluation function

Brenner gradient function is the most straightforward gradient evaluation function, which calculates the square of the gray difference between two adjacent pixels. The function is defined by

$$f(I) = \sum_{x}\sum_{y} [I(x + 2, y) - I(x, y)]^2 \tag{2}$$

Where represents the gray value of image corresponding to pixel point (x, y) and is the calculated result of image clarity.

3.3. Tennengrad evaluation function

The Tenengrad gradient function uses the Sobel operator to extract the horizontal and vertical gradient values, respectively. The image sharpness of the base and Tenengrad gradient function is defined as.

$$f(I) = \sum_{y}\sum_{x} |S(x, y)|, (S(x, y) > T) \tag{3}$$

$$S(x, y) = \sqrt{S_x^2(x, y) + S_y^2(x, y)} \tag{4}$$

where T is the given edge detection threshold, S_x and S_y are the convolution of Sobel horizontal and vertical edge detection operators at pixel points (x, y).

3.4. Energy gradient function

The energy gradient function is similar to the Tenengrad function in that it uses the difference of adjacent points to calculate the gradient value of a point, and the energy gradient function is defined as

$$f(I) = \sum_{x}\sum_{y} \{[I(x + 1, y) - I(x, y)]^2 + [I(x, y + 1) - I(x, y)]^2\} \tag{5}$$

where I(x,y) is the gray value of the image point on (x,y).

4. The automatic focus algorithm based on eight-neighborhood operator and least square planar fitting method

The automatic focus algorithm based on eight-neighborhood operator and least square planar fitting method is presented in this section.

4.1. The process of the proposed automatic focus algorithm

The automatic microscope acquire images used by the automatic focus algorithm based on eight-neighborhood operator, and least square planar fitting method is simply presented as follows. The microscope images referred here are three-dimensional images, and then the points in the planar fitting automatic focus algorithm are defined in the three-dimensional surface.

First, put blood smear into the microscope and start the microscope. The eight-neighborhood operator focusing algorithm proposed in this paper is adopted to focus, scan the images obtained by the low-power microscope, and locate the cell location. After that, turn to the high-power microscope and use the fast focusing algorithm based on eight-neighborhood operator and least square planar fitting method to fit the focal length plane to get the fitting plane. Finally, the cell image was obtained by focusing the cell directly under a low power microscope.

4.2. The process of the automatic microscope acquiring images

Eight-neighborhood operator is presented to focus the low-power microscope cell images automatically here.

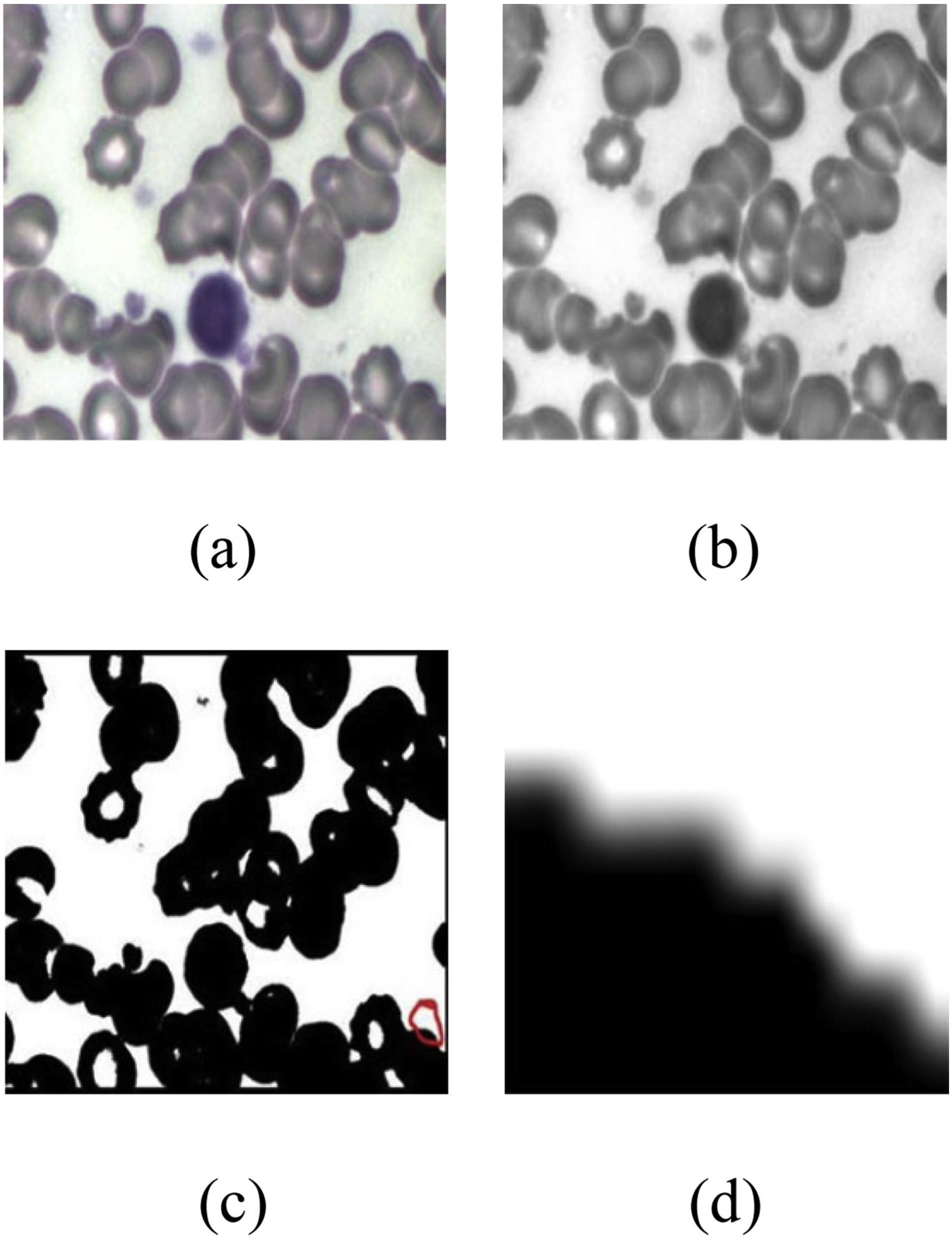

Fig. 1. The original picture (a), the gray scale diagram of the original image (b), the binary image of the original image (c), (d) is the binary image of the selected part in the Fig. 1(c).

4.2.1. Process of automatic focus using the eight-neighborhood operators

The process of the automatic focus using the eight-neighborhood operator is as follows. The relatively clear cell image under the microscope is shown in Fig. 1(a). Firstly the original image is treated by graying. The gray scale image is shown in Fig. 1(b). Then in order to observe the edge information of the microscopic cell image more clearly, the image is transformed into a binary image shown in Fig. 1(c). The binary image with the red circle is shown in Fig. 1(d). The red circle part's pixel values saved in Matlab R2014a is shown in Table 1. The edge information of the red circle part can be seen clearly. The pixel value differences between the pixel in the red circle and the around pixels including its upper pixel, its upper right pixel, and the right pixel are all relatively large. The other information of pixel edge can also be obtained by this method. The eight-neighborhood edge detection and evaluation function are proposed based on the edge information.

4.2.2. Templates of the automatic focus algorithm based on eight-neighborhood operators

An eight-neighborhood operator is proposed combining the characteristics of edge detection information and microscopic blood

Table 1
Binary image pixel values (The red circle part's pixel values saved in MATLAB R2014a.).

x-coordinate y-coordinate	1	2	3	4	5	6	7	8	9	10	11	12	13
1	255	255	255	255	255	255	255	255	255	255	255	255	255
2	255	255	255	255	255	255	255	255	255	255	255	255	255
3	255	255	255	255	255	255	255	255	255	255	255	255	255
4	71	71	163	255	255	255	255	255	255	255	255	255	255
5	0	0	**61**	122	122	188	255	255	255	255	255	255	255
6	0	0	0	0	**0**	87	173	182	247	255	255	255	255
7	0	0	0	0	0	0	**0**	23	201	246	255	255	255
8	0	0	0	0	0	0	0	**2**	18	184	255	255	255
9	0	0	0	0	0	0	0	0	**0**	50	72	127	255
10	0	0	0	0	0	0	0	0	0	0	**0**	37	136
11	0	0	0	0	0	0	0	0	0	0	0	**0**	18

cell image. The eight-neighborhood operator is a template for edge detection and consists of four template blocks of eight-neighborhoods. The template is shown in Fig. 2.

The four templates in Fig. 2 are respectively used to convolve the image. The convolution area d is the difference between the pixel values in the black region and the center pixel. Set the initial value of automatic focus function $F(x) = 0$. If $d \leq n$, $F(x)$ stays the same, otherwise $d > n$, $F(x) = F(x) + 1$.When the maximum value of $F(x)$ is obtained after traversing all images, the position obtained from corresponding images is the focal point of the microscope. The automatic focus function $F(x)$ is shown in Eq.(6). Let $n \in N$ is the threshold. The threshold n can be set according to the characteristics of microscopic blood cell images.

$$F(x) = \begin{cases} F(x),\ d \leq n; \\ F(x) + 1,\ d > n. \end{cases} \tag{6}$$

4.2.3. Computation complexity analysis of eight-neighborhood operator evaluation function

The computation complexity of the eight-neighborhood automatic focus operator evaluation function and other evaluation functions are analyzed. The addition and subtraction times of eight-neighborhood operator and the traditional evaluation functions are compared here.

For a digital image with height H and width W, there is no multiplication and division operation. The subtraction operation of each template is 3, the template movement operation is $(H-1)(W-1)$. For an image with a width of W and a height of H, the number of pairs of operations required by the traditional evaluation function and the evaluation function of eight-neighborhood operators for processing is shown in Table 2. It is clear that the eight-neighborhood operator automatic focus evaluation function

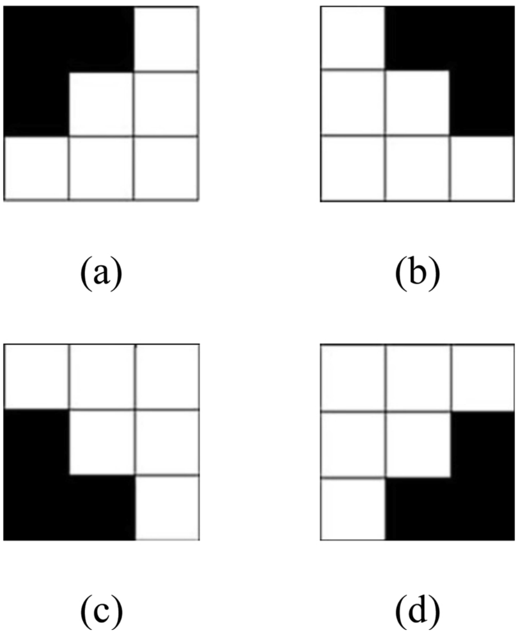

Fig. 2. Four templates for eight-neighborhood operators.

Table 2
Comparison of operation times of each evaluation function.

Function	Multiplication/division times	Add/ subtraction times
Variance	*H*W+1*	*2*H*W*
Brenner	*H*W*	*H*W*
Tennengard	*4*H*W*	*11*H*W*
Energy gradient	*2*H*W*	*3*H*W*
ENOAFEF	*0*	*H*(W-1)*

(ENOAFEF) has the least operation times, and it has the lowest time complexity.

4.3. The automatic focus algorithm based on eight-neighborhood operator and least square planar fitting method

The automatic focus algorithm based on eight-neighborhood operator and least square planar fitting method [24] is concluded as follows steps.

The Automatic focus algorithm

Step 1. Select nine points $A = (x_{1,}, y_{1,}z_{1,}), B = (x_{2,}, y_{2,}z_{2,}), \cdots, I = (x_{9,}, y_{9,}z_{9,})$ from the blood smears, use the eight-neighborhood operator to focus on the nine points, and then acquire the nine focus points denoted as a, b, c…, i.

Step 2. Utilize the nine focal points a, b, c…, i and get the surface Eq. (7) by using the least square planar fitting method[24], and the parameters $a_1, a_2$and a_2 of the surface equation is computed.

$$z = a_0x + a_1y + a_2 \tag{7}$$

Step 3. Save the parameters $a_1, a_2$and $a_3$and the surface equation for the next automatic focus.

5. Experiments

In this section, some experiments, including definition evaluation and microscope cell slide images automatic focusing, are given to show the feasible of the automatic focusing algorithm.

5.1. Definition evaluation experiments

Firstly, the definition evaluation experiments are presented. In the experiments, several groups of blood smear images with gradual resolution under the microscope are used as the automatic focus images. Two groups of image sequences are selected from several groups of blood smear images and used in the experiments. The two image sequences named as image sequences 1 and image sequences 2 are respectively shown as in Figs. 3 and 4. Five evaluation functions, including the variance function, Tennengrad function, energy gradient function, Brenner function, and the proposed eight-neighborhood operators are used in this definition of test experiments. Also, the two image sequences are respectively focused by the five evaluation functions.

The image sequences 1 automatic focus test results by the five evaluation functions $F(x)$ are respectively shown in Fig. 5(a–e). The image sequences 2 automatic focus test results by the five evaluation functions $F(x)$ are respectively shown in Fig. 6(a–e).

5.2. Automatic focus experiments

The microscope cell slide images automatic focus experiments are given in order to verify the proposed automatic focus algorithm in this section. The comparison between the proposed automatic focus algorithm and the artificial vision method is presented here. The artificial vision method means the microscope images are focused through manual observation by the medical staffs.

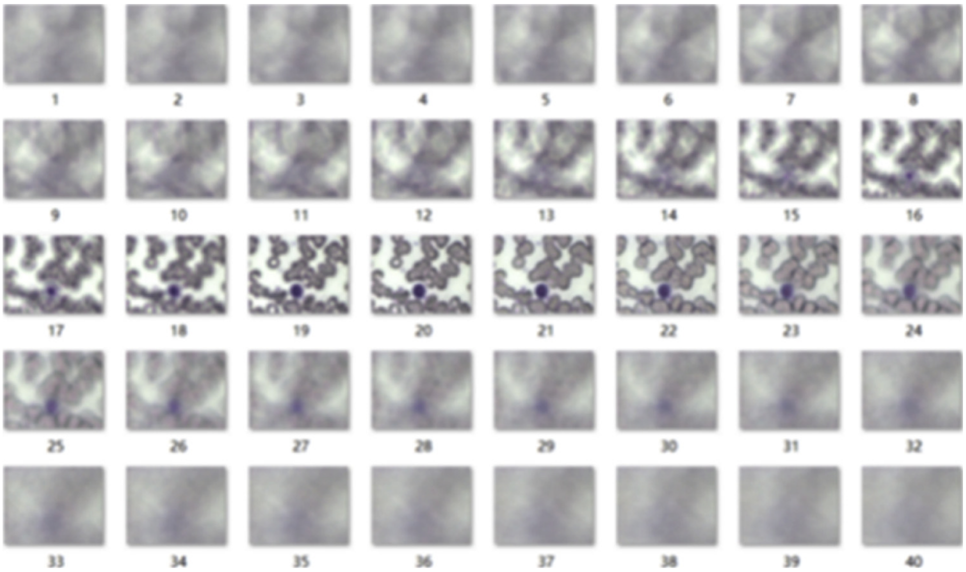

Fig. 3. Image sequences 1.

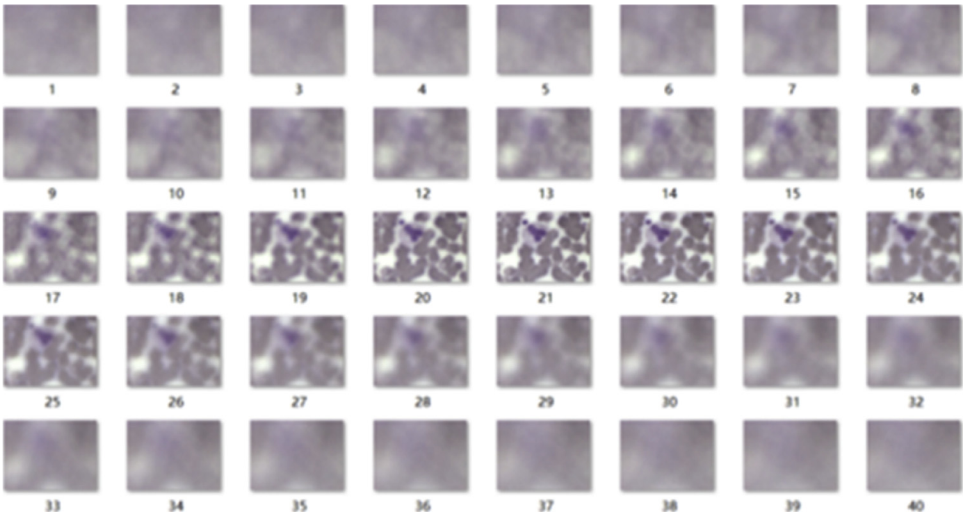

Fig. 4. Image sequences 2.

Twenty microscope cell slide images are selected and respectively focused by the artificial vision and the proposed automatic focus algorithm. The focus image sequences observed by artificial vision are compared with the focus image sequences obtained by the proposed automatic focus algorithm. The automatic focus statistical results by the methods are given in Table 3. In Table 3, F is the results of the focus image sequences observed by the artificial vision, and F(y) is the result of the focus image sequences obtained by the proposed automatic focus algorithm.

In the meanwhile, we compare the auto-focusing time between the proposed eight-neighborhood automatic focus algorithm and the traditional mountain-climbing algorithm. The experimental results is shown in Table 4.

5.3. Discussion

From Figs. 3–6, it's clear that the eight-neighborhood operator evaluation function has a single peak and acuity in the focus of the microscopic cell image. The Ternengrad evaluation function is not suitable for the focus of this kind of image because there are two peaks in the image sequence 1 and an inverted peak in the image sequence 2.

The variance evaluation function is obviously inappropriate for this kind of image. The variance evaluation function has good unimodal property in image sequence 2, but it has the same problem as the Ternengrad evaluation function appearing in image sequence 1. Brenner's evaluation function has good sharpness in image sequence 2, but there are several small peaks. And Brenner's

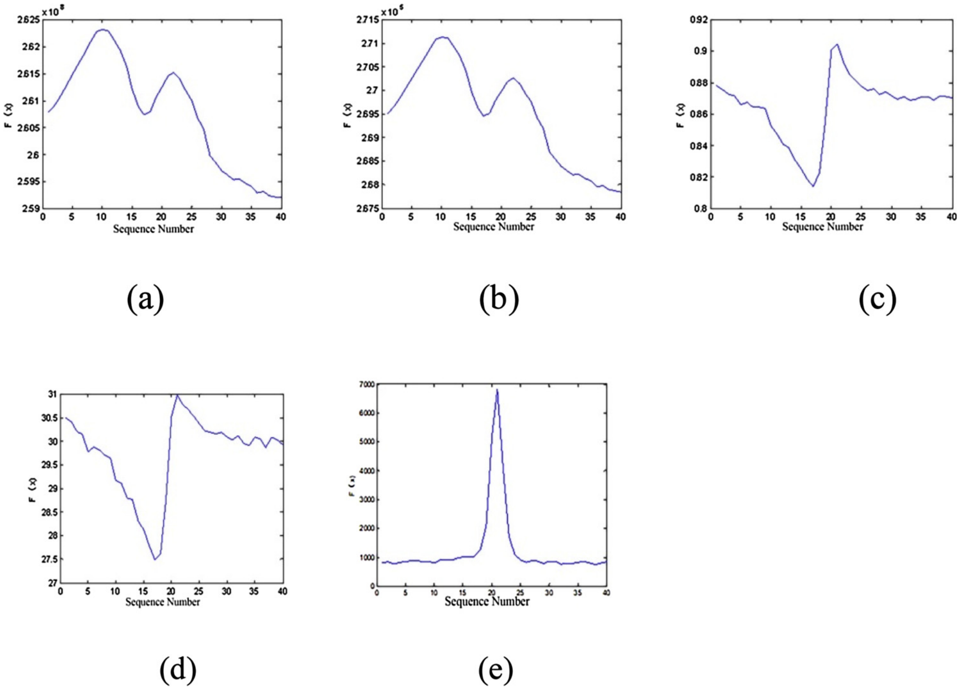

Fig. 5. Sequence Number refers to the number of the corresponding picture in the sequence. The image of Ternengrad evaluation function (a), the image of variance evaluation function (b), the image of Brenner's evaluation function (c), the image of the energy gradient evaluation function (d), the image of the evaluation function of eight-neighborhood automatic focus algorithm (e).

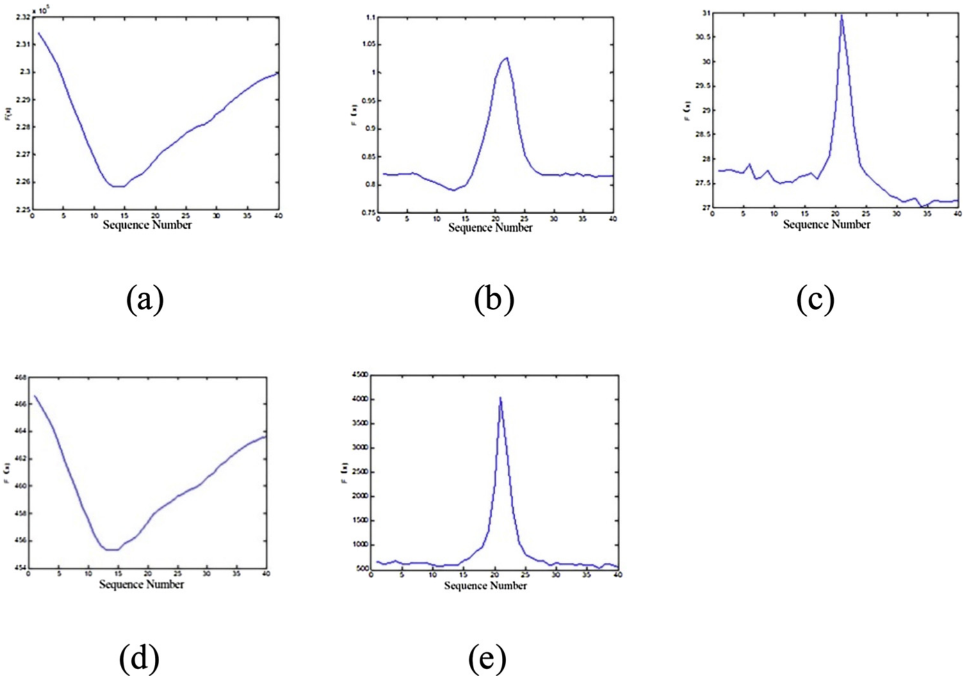

Fig. 6. Sequence Number refers to the number of the corresponding picture in the sequence. The image of Ternengrad evaluation function (a), the image of variance evaluation function (b), the image of Brenner's evaluation function (c), the image of the energy gradient evaluation function (d), the image of the evaluation function of eight-neighborhood automatic focus algorithm (e).

evaluation function doesn't meet the requirements of the definition evaluation function in image sequence 1. It's Obvious that the energy gradient evaluation function performs the worst in the experiments. The eight-neighborhood operator evaluation function outperforms other evaluation functions. The experiments results show that the eight-neighborhood operators are significantly better

Table 3
Automatic focus results by the artificial vision and the proposed automatic focus algorithm.

Results Glass Slide	Artificial Vision(F)	Proposed Algorithm F(y)	ABS(F(y)-F)
Slide 1	20	20	0
Slide 2	22	22	0
Slide 3	21	22	1
Slide 4	22	22	0
Slide 5	21	21	0
Slide 6	20	21	1
Slide 7	21	21	0
Slide 8	21	21	0
Slide 9	21	21	0
Slide 10	21	21	0
Slide 11	20	21	1
Slide 12	20	20	0
Slide 13	21	21	0
Slide 14	21	22	0
Slide 15	21	21	0
Slide 16	21	21	0
Slide 17	22	21	1
Slide 18	21	21	0
Slide 19	21	21	0
Slide 20	20	21	1

Table 4
Comparison of automatic focus time between the proposed eight-neighborhood automatic focus algorithm and the mountain-climbing algorithm.

Algorithm	The Proposed Algorithm	mountain-climbing algorithm
Time/s	3.05	4.06

than other functions in automatic focus micro-fine images. In automatic focusing micro-images, when image of the evaluation function is unimodal or has one peak, it means that there is one focal point and the automatic focusing is successful. When image of the evaluation function is imodal or have two peaks, it means that there are two focal points and the automatic focusing is unsuccessful. When interfered by the impurities on the surface of the thin slice, the function curve shows a very serious local peak and forms a double peak. It is this reason that causes the focusing failure of the traditional algorithm. The eight-neighborhood operator evaluation function fully considers the correlation of adjacent pixels, avoids the influence of impurities on the function curve, and maintains good unimodality.

From Table 3, it is shown that the error range between the fitting degree of plane fitting algorithm and artificial vision is less than an image on average, and this error is within the acceptable range. It's conducted that the plane fitting algorithm is feasible for the automatic focus of microscopic cell images. From Table 4, it is shown that the proposed eight-neighborhood automatic focus algorithm has short time than that of the traditional mountain-climbing algorithm

6. Conclusions

Whether an automatic microscope can obtain high-quality microscopic cell image accurately and quickly greatly depends on the automatic focus function and automatic focus method. An automatic focus algorithm is presented in this paper. The proposed algorithm can focus the cell image under an automatic microscope and improves the edge detection operator according to the edge information of the micro-cell image. More ever, it automatically acquires the micro-cell image under the full-automatic microscope by using the eight-neighborhood automatic focus operator and least square planar fitting method. In this paper, a definition function based on the eight-neighbor operator is proposed. Some simulation experiments and comparison of different definition evaluation functions are given in this paper. It's concluded that the definition evaluation function of the eight-neighborhood operator has its advantages, which not only has good sharpness and single peak but also can be used in actual microscopic cell image automatic focus. In this paper, the traditional mountain-climbing algorithm is not used here for auto-focusing strategy. The eight-neighborhood auto-focusing algorithm is applied according to the characteristics of the slide, which greatly shortens the auto-focusing time of the microscope.

Declaration of Competing Interest

We declare that we have no competing interests.

Acknowledgement

This work is supported by the National Natural Science Foundation of China (Grant No.61402227), Natural Science Foundation of Hunan Province, China (No.2019JJ50618), Degree & Postgraduate Education Reform Project of Hunan Province, China (No.2019JGYB116) and the project of Xiangtan University,Xiangtan, Chian (Grant No.11kz/kz08055). This work is also supported by the key discipline of computer science and technology in Hunan province, China.

Appendix A. Supplementary data

Supplementary material related to this article can be found, in the online version, at doi:https://doi.org/10.1016/j.ijleo.2020.164232.

References

[1] S. Belciug, Machine learning solutions in computer-aided medical diagnosis, Machine Learning for Health Informatics, Springer, 2016, pp. 289–302.
[2] L. Yu, R. Wang, J. Zhou, B. Xu, Rapid acquisition of high-volume microscopic images using predicted focal plane, J. Microsc. 263 (2016) 320–327.
[3] J. Vargas, E. Franken, C. Sorzano, J. Gomez-Blanco, R. Schoenmakers, A. Koster, J. Carazo, Foil-hole and data image quality assessment in 3DEM: towards high-throughput image acquisition in the electron microscope, J. Struct. Biol. 196 (2016) 515–524.
[4] J.S. Lim, G.D. Wright, B. Burke, W. Xie, A user-interactive algorithm quantifying nuclear pore complex distribution within the nuclear lamina network in single molecular localization microscopic image, Methods 157 (2019) 42–46.
[5] H.-C. Choi, C.S.K. Kim, R. Tarran, Automated acquisition and analysis of airway surface liquid height by confocal microscopy, Am. J. Physiol.-Lung Cell. Mol. Physiol. 309 (2015) L109–L118.
[6] E.O. Fernandez, M. Nilo, J.O. Aquino, J.M.P. Bravo, S. Julie-Anne, C.V.B. Gaddi, C.A. Simbran, Microcontroller-based automated microscope for image recognition of Four urine constituents, TENCON 2018-2018 IEEE Region 10 Conference, IEEE, 2018, pp. 1689–1694.
[7] Y. Lei, Z. Yao, D. He, Design and experiment of a remote acquisition system for wheat spore microspore summer spore microscopic images, J. Agric. Mach. (2018) 39–47.
[8] C.T. Liu, Z.X. He, Y. Zhan, H.C. Li, Searching algorithm of theodolite auto-focusing based on compound focal judgment, EURASIP J. Wirel. Commun. Netw. 2014 (2014) 110.
[9] Y. Liu, Q. Xu, Design of a flexure-based auto-focusing device for a microscope, Int. J. Precis. Eng. Manuf. 16 (2015) 2271–2279.
[10] S. Liu, M. Liu, Z. Yang, An image auto-focusing algorithm for industrial image measurement, EURASIP J. Adv. Signal Process. 2016 (2016) 70.
[11] F.S. Zhang, S.W. Li, Z.G. Hu, Z. Du, Fish swarm window selection algorithm based on cell microscopic automatic focus, Cluster Comput. 20 (2017) 1–11.
[12] X. Zhang, F. Zeng, Y. Li, Y. Qiao, Improvement in focusing accuracy of DNA sequencing microscope with multi-position laser differential confocal autofocus method, Opt. Express 26 (2018) 887–896.
[13] C.C. Gu, H. Cheng, K.J. Wu, L.J. Zhang, X.P. Guan, A high precision laser-based autofocus method using biased image plane for microscopy, J. Sens. 2018 (2018) 1–6.
[14] N. Nguyen, K. Doğançay, H.-T. Tran, P. Berry, An image focusing method for sparsity-driven radar imaging of rotating targets, Sensors 18 (2018) 1840.
[15] H. Dogan, M. Ekinci, Automatic panorama with auto-focusing based on image fusion for microscopic imaging system, Signal Image Video Process. 8 (2014) 5–20.
[16] E.M.D.S. Santos, A.R.S. Marcal, Automatic identification of pollen in microscopic images, European Congress on Computational Methods in Applied Sciences & Engineering (2017).
[17] Y. Zhang, W. Wei, Y. Yuan, Multi-focus image fusion with alternating guided filtering, Signal Image Video Process. (2018) 1–9.
[18] M.I. Shah, S. Mishra, M. Sarkar, C. Rout, Identification of robust focus measure functions for the automated capturing of focused images from Ziehl-Neelsen stained sputum smear microscopy slide, Cytom. Part A (2020).
[19] Y. Zhang, S. Ji, Q. Wang, BrennerImage sharpness evaluation algorithm based on region contrast, Appl. Opt. 33 (2012) 6.
[20] J. Guo, W. Zeng, T. Xie, A fast automatic focusing method based on entropy function, Measuring Tech. (2003) 30–32.
[21] C. Mo, B. Liu, L. Ding, E. Chen, G. Guo, A gradient threshold auto-focus algorithm, Infrared Laser Eng. (2014).
[22] L. Bai, M. Xu, Study on automatic focusing method of microscope based on image processing, Chin. J. Sci. Instrum. 20 (1999) 612–614.
[23] G.E. Hinton, Learning multiple layers of representation, Trends Cogn. Sci. 11 (2007) 428–434.
[24] M. Kesäniemi, K. Virtanen, Direct least square fitting of hyperellipsoids, IEEE Trans. Pattern Anal. Mach. Intell. 40 (2017) 63–76.